Journal of Power Sources, 43–44 (1993) 269–275

Electrodes for lithium batteries

J. B. Goodenough, A. Manthiram and B. Wnetrzewski

Center for Materials Science and Engineering, ETC 9.102, University of Texas at Austin, Austin, TX 78712 (USA)

Abstract

The several constraints imposed on the selection of electrode materials for a secondary lithium battery are reviewed. Some structural and electronic considerations that must be taken into account in the design of an electrode material are discussed.

Introduction

A lithium battery may be represented as:

$$S^+/L \text{ or } P/S^- \quad (1)$$

where S^+ is the positive (cathode) and S^- is the negative (anode) solid electrode. The liquid (L) or polymer (P) Li^+ ion electrolyte contains a separator permeable to the electrolyte.

Figure 1 illustrates a schematic energy diagram at open circuit; Φ_A and Φ_C represent, respectively, the anode and cathode work functions; the open-circuit voltage is:

$$V_{0c} = (\Phi_A - \Phi_C)/e_0 \quad (2)$$

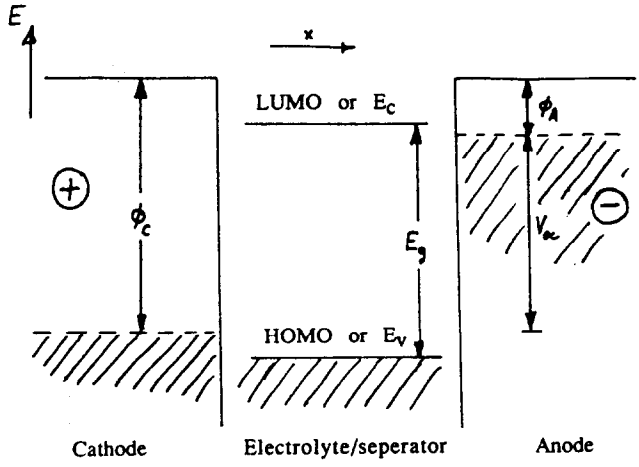

Fig. 1. Cell at open circuit.

0378-7753/93/$6.00

where e_0 is the magnitude of the electronic charge. Thermodynamic stability constrains the electrode Fermi energies E_F to lie within the energy gap E_g of the electrolyte, but kinetic barriers may allow this constraint to be relaxed somewhat.

Ideally, it would be preferable to have elemental Li as the anode and, as the cathode, an insertion compound into which Li can be inserted/extracted reversibly over a large solid-solution range with little change in Φ_C. Such a concept was demonstrated a number of years ago [1] with the cell:

$$Li_xTiS_2/L/Li \quad 0<x<1 \tag{3}$$

Problems with the Li anode have motivated a search for an alternate anode material that is stable against the existing electrolytes, but with the smallest possible increase in the anode work function ϕ_A. One solution would be an insertion compound for the anode as well as the cathode; the lithiated carbon electrodes illustrate this approach.

An increase in Φ_A requires an equivalent increase in Φ_C if a suitably high V_{oc} is to be maintained. It was this realization that originally [2] motivated a study of alternative cathode materials; the 'rocking-chair' cell [3]:

$$Li_x[Mn_2]O_4/LiClO_4+PC/Li_xC \tag{4}$$

represents a follow through of this fundamental idea.

Structural considerations

An insertion compound consists of a **host** matrix into/from which a **guest** species may be inserted/extracted **reversibly** without a rearrangement of the host structure. Two general classes of host structures have been studied: layered hosts and framework hosts. The layered hosts consist of layers of strongly-bonded atoms that are held together by weak interlayer bonding. These hosts support two-dimensional (2D) motion of the guest species between the layers; a flexible interlayer spacing allows a facile accommodation of changes in the interlayer bonding with guest concentration.

Framework hosts allow 1D insertion into parallel tunnels, 2D insertion into multidirectional tunnels that intersect within a plane, or 3D insertion. The 1D tunnel structures, such as the hexagonal tungsten bronzes or α-MnO_2, have their tunnels readily blocked by shear defects or large foreign ions; mismatch across grain boundaries can also be a problem. Of more interest are the 2D and 3D framework hosts.

Figure 2 illustrates the structures of the layered oxides $LiMO_2$ (M = V, Cr, Co, or Ni) and the spinels $A[B_2]X_4$. The layered oxides have a structure analogous to that of $LiTiS_2$, but the sulfide ions of $LiTiS_2$ are hexagonal-close-packed. In the layered oxides, the Li and M atoms occupy alternate (111) planes of the rocksalt structure. In the spinel structure, the empty octahedral sites 16*c* form an array like that of the occupied 16*d* sites, but displaced by half a cubic lattice parameter; they share common faces with the occupied tetrahedral sites 8*a* and common edges with one another to form an interstitial space continuously connected in 3D. In the spinels $Li[B_2]X_4$, e.g., $Li[Mn_2]O_4$ and $Li[Ti_2]S_4$, the Li atoms occupy this interstitial space, and it is possible to insert or extract Li at room temperature to obtain $Li_x[B_2]X_4$ ($0 \leqslant x \leqslant 1$) without disrupting the $[B_2]X_4$ array.

In the layered compounds, flexibility of the interlayer spacing allows insertion between the layers of species other than Li from the electrolyte. Insertion of unwanted species over time blocks access of Li to the electrode and thus reduces its capacity. The dimensions of the spinel hosts, on the other hand, are held rigid in 3D by strong B–X bonding, so only Li has access to the interstitial space.

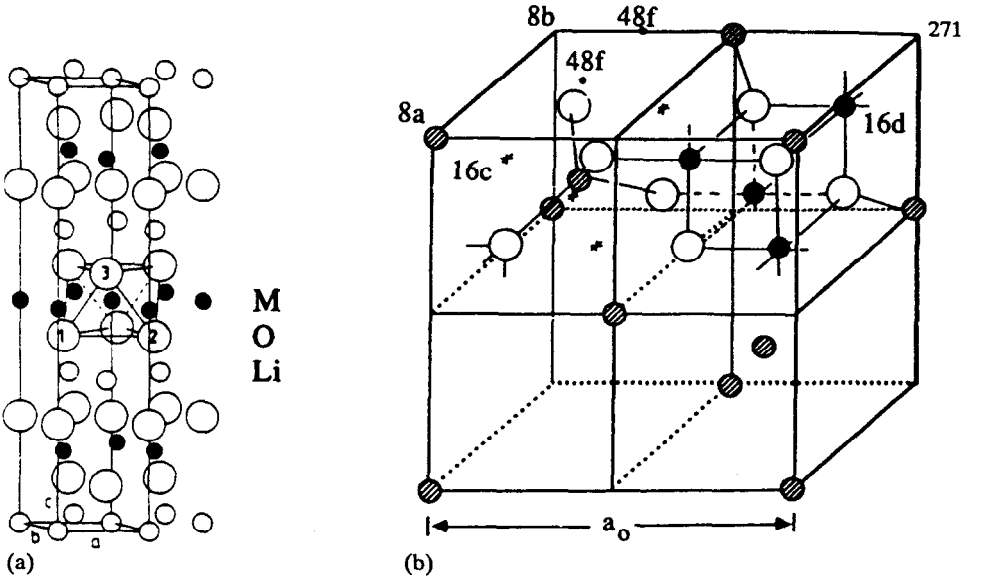

Fig. 2. (a) $LiMO_2$ structure, and (b) spinel structure.

In the layered oxides $LiMO_2$, the O–M–O layers are bonded electrostatically via the interlayer Li^+ ions. Extraction of Li in $Li_{1-y}MO_2$ reduces the interlayer bonding so the spacing between the layers increases; at higher values of y, the layers repel one another unless there is either a displacement of M atoms from the M layers to the Li planes or cooperative ionic movements within the layers along the c-axis that create dipolar interlayer coupling. The critical value of y at which M-atom displacements occur varies with the M atom. In $Li_{1-y}VO_2$, the V atoms become displaced for $y > 0.33$. In the case of $Li_{1-y}CoO_2$, intralayer ionic movements stabilize the layered structure to higher values of y. In the sulfides, van der Waals bonding between the S–M–S layers stabilize a layered structure even in the absence of Li^+ ions. In fact, the Li^+ ions can only enter the empty octahedral sites by prizing apart the sulfide planes. Therefore the Li^+ ions have a lower mobility in the Li_xMS_2 compounds than they do in $Li_{1-y}CoO_2$ compounds [4].

The situation is just the opposite in the spinel structure. In cubic $Li_x[Ti_2]S_4$, the octahedral-site preference of a Li^+ ion is strong enough to overcome the electrostatic interactions favoring tetrahedral-site occupancy, so the Li^+ ions move in the interstitial 16*c* octahedral-site array as in the layered compounds and V_{oc} versus x is nearly the same for both structures [5]. Even though the spinel dimensions are constrained in 3D, the Li^+ ion mobility is also essentially the same as that in the layered Li_xTiS_2. In the oxides, on the other hand, the smaller lattice parameter and the lower anion polarizability reduce the Li^+ ion mobility significantly at room temperature. Moreover, stronger electrostatic forces tend to order the Li^+ ions onto tetrahedral sites, which changes the V_{oc}.

Electronic considerations

Mixed-valent electronic mobilities

In both the layered and spinel structures, the transition-metal cations occupy octahedral sites. Moreover, both the layered and spinel phases have only 90° M–O–M

or B–O–B interactions; there are no 180° interactions. In this situation, the σ-bonding e orbitals on neighboring cations are orthogonal to one another, so they have little bandwidth. On the other hand, the π-bonding t_2 orbitals (a_1 and e_π due to trigonal component of crystalline field) of neighboring transition-metal cations do overlap one another to give a π^* band associated with metal–metal interactions across a shared octahedral-site edge. In the spinels $Li[Ti_2]X_4$, X = O or S, the Ti–Ti interactions are strong enough to make itinerant any d electrons on the Ti-atom array; these compounds are metallic. In the spinel $Li[Mn_2]O_4$, on the other hand, the Mn–Mn interactions are too weak to give an itinerant-electron bandwidth, so the t_2^3 configuration is localized and magnetic. But of more interest for the electrical conductivity is the partially occupied e-orbital configuration; the high-spin $Mn^{3+}:t_2^3e^1$ and $Mn^{4+}:t_2^3e^0$ configurations coexist, but with 90° Mn–O–Mn interactions the e electrons remain localized. In the mixed-valent regime, they become trapped in local lattice relaxations, so their mobility carries an activation energy. Consequently $Li[Mn^{4+}Mn^{3+}]O_4$ is a 'small-polaron' semiconductor, not a metal, whereas $Li[Ti_2]O_4$ is a superconductor. In any analysis of electrochemical data, small polarons must be treated statistically as counter anions [6]; but itinerant electrons are not to be treated in this way.

Tailoring the work function

Figure 3 shows a schematic construction of the electronic energy levels of MnO from the perspective of an ionic model. The energy marked 'Vac' is the lowest vacuum energy. E_I is the energy lost to remove an electron from a Mn^+ ion to an O^- ion at infinite separation so as to create a Mn^{2+} and an O^{2-} ion. On assembling the ions to form a crystalline array of point charges, the system gains the coulombic Madelung energy E_M. Conservation of energy causes E_M to lower the $O^{2-}:2p^6$ level and raise the $Mn^{2+}:4s$ level. An $E_M > E_I$ is required to stabilize ionic bonding.

E_M also raises the energy of the localized $Mn^{2+}:3d^5$ manifold above the $O^{2-}:2p^6$ level, placing it in the energy gap between the $Mn^{2+}:4s$ and $O^{2-}:2p^6$ bands. An e electron is removed from the $Mn^{2+}:t_2^3e^2$ configuration to create a high-spin $Mn^{3+}:t_2^3e^1$ ion on oxidation; therefore, the $Mn:3d^5$ energy level corresponds to the $Mn^{3+/2+}$ redox energy.

Because the 3d electrons are 'localized', successive redox couples are separated by discrete energies; the separation between the $Mn^{3+/2+}:3d^5$ and $Mn^{2+/+}:3d^6$ energies is large because the high-spin $3d^5$ configuration already has one electron in each 3d

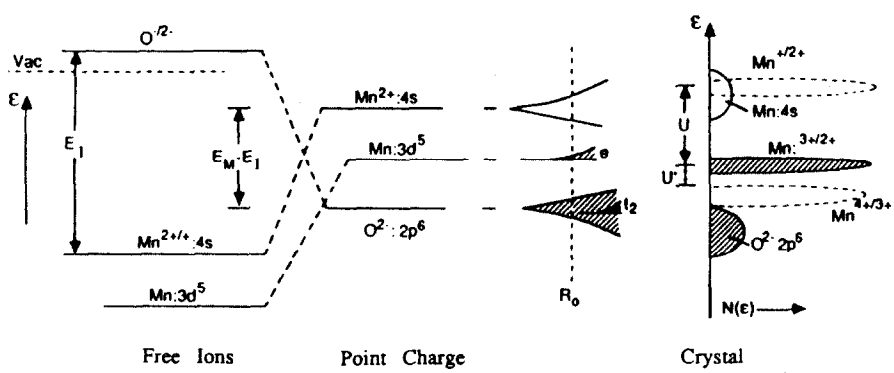

Fig. 3. Schematic ionic-model derivation of electron energies in MnO.

orbital. On the other hand, removal of an electron from a half-filled e orbital to create $Mn^{3+}:t_2^3e^1$ changes the intraatomic electron-electron electrostatic energy by a relatively small amount, so the separation of the $Mn^{3+/2+}:3d^5$ and $Mn^{4+/3+}:3d^4$ redox couples is relatively small. In fact, the Mn^{4+} ion is chemically accessible in the octahedral site of an oxide.

The sulfide ions have a more negative electron affinity than the oxide ions, so E_I is larger for MnS than for MnO. Moreover, the larger sulfide ion makes a larger lattice parameter, and hence a smaller E_M, in MnS. As a result, E_M is only large enough to raise the $Mn^{3+/2+}:3d^5$ redox couple to the top of the $S^{2-}:3p^6$ band, and a Mn^{4+} valence state is not accessible chemically in the sulfides. Attempts to oxidize manganese to the Mn^{4+} state in a sulfide result in holes in the $S^{2-}:3p^6$ band, and these holes are trapped out in S–S bonds by the formation of $(S_2)^{2-}$ ions. Clearly a lower Fermi energy E_F and hence a larger cathode work function Φ_C can be obtained in an oxide than in a sulfide.

This concept is illustrated in Fig. 4, which illustrates schematically the density $N(E)$ of one-electron energies versus energy E for the two layered compounds Li_xTiS_2 and $Li_{1-y}CoO_2$. The conduction band in TiS_2 nearly overlaps the top of the $S^{2-}:3p^6$ band. Any increase in Φ_C significantly within a sulfide must be constrained by a lowering of E_F into the $S^{2-}:3p^6$ band, which will tend to be unstable relative to the formation of $(S_2)^{2-}$ ions. It is this situation that led some years ago to an investigation of the layered oxides [2].

In the case of $LiCoO_2$, the low-spin $Co(III):t_2^6e^0$ configuration places E_F between a filled π^* band of t_2^6 parentage and an empty σ^* band of e^0 parentage. Removal of Li from the semiconductor $LiCoO_2$ introduces mobile holes into the π^* bands, which are strongly covalent with a nearly equal mixture of O-2p and Co-t_2 character. However, the point to be emphasized here is that the oxide matrix allows a larger E_M–E_I and hence access to higher formal cation valence states; this access allows the development of cathode materials having a $V_{oc} > 4$ eV relative to a Li anode [2].

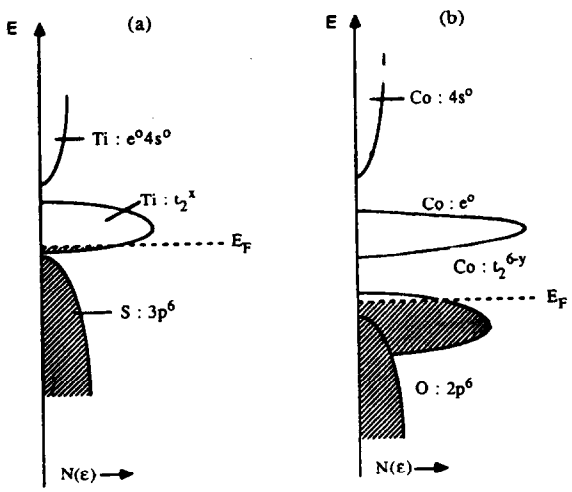

Fig. 4. Schematic energy vs. density of states for (a) Li_xTiS_2, and (b) $Li_{1-y}CoO_2$.

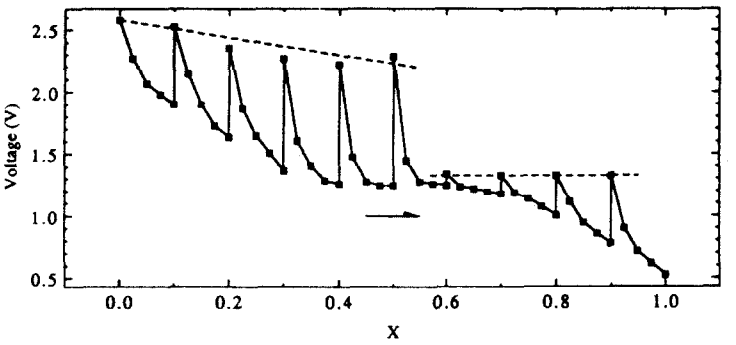

Fig. 5. Interrupted discharge curve $Li_{1+x}[Ti_2]O_4/Li$.

Influence of lithium distribution

The dependence of the open-circuit voltage V_{oc} on Li concentration x in Li_xTiS_2 can, as mentioned above, be accounted for with a statistical distribution of the Li^+ ions over the octahedral sites available to them. A similar V_{oc} versus x-curve is found in the cubic $Li_x[Ti_2]S_4$ spinel system [5, 7], which indicates that here also there is a statistical distribution of Li^+ ions over the 16*c* octahedral sites. The relatively strong octahedral-site preference of a Li^+ ion in a close-packed sulfide-ion array makes it necessary first to prepare indirectly the $[B_2]S_4$ framework [5, 8]. Lithium atoms inserted into these $[B_2]S_4$ frameworks occupy only 16*c* octahedral sites.

The situation is quite different in the oxospinels, which can be obtained by direct chemical synthesis. $Li[Ti_2]O_4$ is a conventional metal. Extraction of Li from the tetrahedral sites is possible only to $Li_{0.8}[Ti_2]O_4$; chemical lithiation of $Li_{0.8}[Ti_2]O_4$ results in a two-phase system between the spinel and the ordered rocksalt $Li[Ti_2]O_4$. The reported [9] discharge voltage V versus x for $Li_{1+x}[Ti_2]O_4$, $-0.2 \leqslant x \leqslant 1.0$, is a nearly flat $V=$ 1.3 V in the interval $0 < x < 1.0$. However, Fig. 5 shows the V versus x variation if the discharge curve is interrupted at successive intervals and allowed to relax to an equilibrium V_{oc}. Although sufficient time to reach complete equilibrium was not taken between discharge steps, it is clear that there is a step of over a volt in the equilibrium V_{oc} on passing through the composition $Li_{1.5}[Ti_2]O_4$. The voltage V versus Li anode decreases sharply (the work function Φ_C decreases) on transfer of the Li^+ ions from tetrahedral to octahedral sites. Under steady-current conditions, the coexistence of a spinel phase in the interior of the particle and a rocksalt phase penetrating from the surface leads to a constant discharge voltage $V \approx 1.3$ V. On charging, the spinel structure is retrieved at $x=0$ with all the Li^+ ions in tetrahedral sites. However, if the discharge is interrupted, an intermediate phase at $x=1.5$ becomes established by a slow rearrangement of the Li^+ ions. The most probable configuration is one where the Li^+ ions become arranged in pairs sharing a face common to a tetrahedral and an octahedral site.

In the manganese oxides with spinel frameworks $[Mn_{2-y}Li_y]O_4$, the open-circuit voltage versus Li is about 3 V where the inserted Li occupy octahedral 16*c* sites, but may be in excess of 4 V where they partially occupy tetrahedral 8*a* sites.

Acknowledgements

We gratefully acknowledge the support of the Welch Foundation, Houston, TX.

References

1 M. S. Whittingham, *Science, 92* (1976) 1126; *Prog. Solid State Chem., 12* (1978) 41.
2 K. Mizushima, P. C. Jones, P. J. Wiseman and J. B. Goodenough, *Mater. Res. Bull., 17* (1980) 785.
3 D. Guyomard and J. M. Tarascon, personal communication.
4 M. G. S. R. Thomas, P. G. Bruce and J. B. Goodenough, *Solid State Ionics, 17* (1985) 13.
5 A. C. W. P. James and J. B. Goodenough, *Solid State Ionics, 27* (1988) 37.
6 J. B. Goodenough, in B. Schumann, Jr. (eds.), *Proc. Symp. Manganese Dioxide Electrode,* Proc. Vol. 85-4, The Electrochemical Society, Pennington, NJ, USA, 1985, p. 77.
7 S. Sinha and D. W. Murphy, *Solid State Ionics, 20* (1986) 81.
8 A. Manthiram and J. B. Goodenough, *J. Solid State Chem., 71* (1987) 349.
9 K. M. Colbow, J. R. Dahn and R. R. Haering, *J. Power Sources, 26* (1989) 397.